MATHEMATICS OF COMPUTATION
Volume 00, Number 0, Pages 000–000
S 0025-5718(XX)0000-0

OPTIMAL FILTER AND MOLLIFIER FOR PIECEWISE SMOOTH SPECTRAL DATA

JARED TANNER

This paper is dedicated to Eitan Tadmor for his direction.

ABSTRACT. We discuss the reconstruction of piecewise smooth data from its (pseudo-) spectral information. Spectral projections enjoy superior resolution provided the function is globally smooth, while the presence of jump discontinuities is responsible for spurious $\mathcal{O}(1)$ Gibbs' oscillations in the neighborhood of edges and an overall deterioration of the convergence rate to the unacceptable first order. Classical filters and mollifiers are constructed to have compact support in the Fourier (frequency) and physical (time) spaces respectively, and are dilated by the projection order or the width of the smooth region to maintain this compact support in the appropriate region. Here we construct a non-compactly supported filter and mollifier with optimal *joint* time-frequency localization for a given number of vanishing moments, resulting in a new fundamental dilation relationship that adaptively links the time and frequency domains. Not giving preference to either space allows for a more balanced error decomposition, which when minimized yields an optimal filter and mollifier that retain the robustness of classical filters, yet obtain true exponential accuracy.

1. INTRODUCTION

The Fourier projection of a 2π periodic function $S_N f(\cdot)$, enjoys the well known spectral convergence rate, that is, the convergence rate is as rapid as the *global* smoothness of $f(\cdot)$ permits. Specifically, if $f(\cdot)$ has s bounded derivatives then $|S_N f(x) - f(x)| \leq Const \|f\|_{C^s} \cdot N^{1-s}$, and if $f(\cdot)$ is analytic, $|S_N f(x) - f(x)| \leq Const \cdot e^{-\eta_f N}$. In the dual (frequency) space the global smoothness and spectral convergence are reflected in rapidly decaying Fourier coefficients $|\hat{f}_k| \leq 2\pi k^{-s} \|f\|_{C^s}$. On the other hand, spectral projections of piecewise smooth functions suffer from the well known Gibbs' phenomena, where the uniform convergence of $S_N f(x)$ is lost in the neighborhood of discontinuities. Moreover, the *global* convergence rate of $S_N f(x)$ deteriorates to first order. Two interchangeable processes for recovering the rapid convergence associated with globally smooth functions are mollification, $\psi(\cdot)$, in the physical space and filtering, $\sigma(\cdot)$, in the dual space,

$$\psi(x) := \frac{1}{2\pi} \sum_{k=-\infty}^{\infty} \sigma\left(\frac{k}{N}\right) e^{ikx},$$

where the filter is traditionally supported in $[-1, 1]$ and dilated by the projection order, N. When viewed as operating in the Fourier dual space, filtering accelerates convergence by premultiply the Fourier coefficients $\hat{f}_k$ by a smoothly decreasing function, $\sigma(\cdot)$, resulting in modified coefficients $\hat{f}_k \sigma(k/N)$ with a greatly accelerated decay rate as $|k| \uparrow N$. For filters the smoothness in the dual space corresponds to localization in the physical (time) space, exhibited through the action of the filter's associated mollifier, $\psi(\cdot)$. Customarily mollifiers have been defined to have compact support in the physical space, $\psi(x) = 0$ for $|x| \geq \pi$; and the error after mollifying a function's spectral projection is analyzed in terms of the competing dual space localization error, and accuracy error which is controlled by a number of (near) vanishing moments possessed by the mollifier,

$$\int_{-r}^{r} x^j \psi(x) dx \sim \delta_{j0} \qquad j = 0, 1, \ldots, p-1.$$

Alternatively, filters have traditionally been defined to have compact support in the Fourier dual space, $\sigma(\xi) = 0$ for $|\xi| \geq 1$, and the error after filtering a function has been decomposed into a competing physical

Received by the editor May 18, 2004 and, in revised form, .
1991 *Mathematics Subject Classification.* 41A25, 42A10, 42A16, 42A20, 42C25, 65B10, 65T40.
Key words and phrases. Fourier series, filters, time-frequency localization, piecewise smooth, spectral projection.
The author was supported in part by NSF Grant #DMS01-35345.

space localization error and an accuracy error, which is again directly related to the (near) vanishing moments of the filter's associated mollifier, through the classical filter accuracy condition,

$$\sigma^{(j)}(0) \sim \delta_{j0} \qquad j = 0, 1, \ldots, q-1. \tag{1.3}$$

The restriction of compact support in either the physical or Fourier dual space does not permit analytic mollifiers or filters, and as a results limits their time-frequency localization. In [17] and [18] a somewhat less regular space[1] was utilized to derive root-exponential convergence by balancing the competing errors through linking the mollifier and filter orders,p and q respectively, to the degree of the function's spectral projection, N, and the distance from the point being recovered to the nearest discontinuity, $d(x)$. Although compact support in either of the physical or dual space is desirable in some instances, as discussed in §5; to achieve minimal error neither space has priority and the filter or mollifier should possess the optimal joint time-frequency localization for a given number of near vanishing moments. Here a mollifier and filter are introduced which, for a given accuracy, possess optimal joint localization in both spaces as measured by the classical uncertainty principle[2]

$$4\pi \|xg(x)\|_{L^2} \cdot \|\xi(\mathcal{F}g)(\xi)\|_{L^2} \geq \|g\|_{L^2}^2. \tag{1.4}$$

Rather than maximizing the overall localization, in order to maintain compact supported in the domain of the Fourier projection, $[-N, N]$, or region of smoothness in the physical space, $[x - d(x), x + d(x)]$, filters and mollifiers have been dilated by N and $d(x)$ respectively. Yet, for filtering and mollification to be performing the same action in the two spaces, the Fourier transform would imply that their dilation factors would be the inverse of one another. In §2 a new error decomposition applicable for non-compactly supported filters and mollifiers is formulated, separated into the classical accuracy error as well as competing physical and dual space localization errors. By balancing the joint time-frequency localization for the region $[x - d(x), x + d(x)] \times [-N, N]$ a new fundamental scaling factor is determined, $\sqrt{N/d(x)}$ and its inverse for the dual and physical spaces respectively. The resulting optimal filter and mollifier introduced in §3 and §4, achieve substantially improved convergence rates over classical filters and mollifiers as stated in Theorems 3.2 and 4.2, and exhibited in the numerical examples, §5. Additionally, similar to [17] and [18] the adaptive optimal number of near vanishing moments is determined for this scaling relation, balancing the overall error.

2. Non-compact Filters and Mollifiers

We begin with the classical filter dilation N, and consider general analytic filter $\sigma(\cdot)$, mollifier $\psi(\cdot)$, pairs that are jointly well localized in both the dual Fourier and physical space. Although equivalent, filters are viewed as operating in the Fourier dual space,

$$S_N f^\sigma(x) := \sum_{|k| \leq N} \sigma\left(\frac{k}{N}\right) \hat{f}_k e^{ikx} \qquad \hat{f}_k := \frac{1}{2\pi} \int_{-\pi}^{\pi} f(x) e^{-ikx} dx, \tag{2.1}$$

and mollifiers acting under convolution in the physical space,

$$S_N f^\sigma(x) \equiv \psi * S_N f(x) = \int_{-\pi}^{\pi} \psi(y) f(x-y) dy \qquad \psi(x) := \frac{1}{2\pi} \sum_{k=-\infty}^{\infty} \sigma\left(\frac{k}{N}\right) e^{ikx}. \tag{2.2}$$

Although the filter may not be compactly supported, when applied to a function's spectral projection, only the low modes participate, $|k| \leq N$, and as such, the mollifer's definition may similarly be formulated using only those elements of the filter. The error after mollification (filtering) is traditionally decomposed as

$$\begin{aligned} E(N, q, x) &:= f(x) - \psi * S_N f(x) \\ &= (f(x) - \psi * f(x)) + (\psi - S_N \psi) * (f(x) - S_N f(x)) \\ &=: R(N, q, x) + L_D(N, q, x) \end{aligned} \tag{2.3}$$

which we refer to as the regularization and dual space localization errors respectively. Although the second term of (2.3) is a measure of the mollifier's dual space localization, it has traditionally been labeled the

[1] A function $\rho(\cdot)$ is in Gevrey regularity α if $\|\rho^{(s)}\|_{L^\infty} \leq K_\rho (s!)^\alpha \eta_\rho^{-s}$ for some K_ρ, η_ρ independent of s. Analytic functions satisfy $\alpha = 1$, and compactly supported functions can at most satisfy $\alpha > 1$.

[2] For consistency with the Fourier series expansion used here, (2.1), we use the Fourier transform normalization $(\mathcal{F}g)(\xi) := \frac{1}{2\pi} \int_{-\infty}^{\infty} e^{ix\xi} g(x) dx$; and note that equality in (1.4) is satisfied if and only if $g(x) = \exp(-cx^2)$ for $c > 0$.

truncation error, as it is the error introduced by truncating the mollifier's spectral representation, [10]. The regularization error can be further decomposed into the accuracy and physical space localization errors,

$$\begin{aligned} R(N,q,x) &= \int_{|y|\le r}[f(x)-f(x-y)]\psi(y)dy + \int_{r\le|y|\le\pi}[f(x)-f(x-y)]\psi(y)dy \\ &=: A(N,q,x)+L_P(N,q,x). \end{aligned}$$

The physical space localization error is determined by the decay of the mollifier for $|y| \ge r$, which is a consequence of the associated filter's smoothness; and the accuracy error is controlled by both the localization of the mollifier, as well as the number of (near) vanishing moments possessed by the mollifier. Combining these components, the total error is composed of the localization and the accuracy errors,

$$E(N,q,x) := L_D(N,q,x)+L_P(N,q,x)+A(N,q,x). \tag{2.4}$$

Classical compactly supported mollifiers and filters enforce $L_P = 0$ and $L_D = 0$ respectively, with compact support in both spaces simultaneously excluded[3], [12]. Alternatively, the minimal total error is achieved by balancing the three competing errors in (2.4). In lieu of carrying out the analysis for a general smooth (analytic) filter, or (exponentially) well localized mollifier, we focus on a specific filter mollifier pair that possess optimal joint time-frequency localization, and which allows for an increasing number of near vanishing moments. The Distributed Approximating Hermite Functionals, DAHF, introduced in [13] are such a class of functions and we catalog some of their properties in the following lemma.

Lemma 2.1. *The p order DAHF is given by*

$$\phi_{p,\gamma}(x) := e^{-x^2/(2\gamma^2)}\gamma^{-1}\sum_{n=0}^{p}\frac{(-4)^{-n}}{n!}H_{2n}\left(\frac{x}{\gamma\sqrt{2}}\right), \tag{2.5}$$

where H_{2n} is the Hermite polynomial of order $2n$, and the DAHF's Fourier transform is given by

$$(\mathcal{F}\phi_{p,\gamma})(\xi) := e^{-\xi^2\gamma^2/2}\sum_{n=0}^{p}\frac{(\xi^2\gamma^2)^n}{2^n n!}. \tag{2.6}$$

Let $\delta\phi_{p,\gamma} := [\phi_{p,\gamma}-\phi_{p-1,\gamma}]$ be the difference between consecutive order DAHFs, and expand the time-frequency uncertainty for $\phi_{p,\gamma}$ in terms of the increase in frequency (dual) space uncertainty

$$\|x\phi_{p,\gamma}(x)\|_{L^2}^2\left(\|\xi(\mathcal{F}\phi_{p-1,\gamma})(\xi)\|_{L^2}^2+\|\xi(\mathcal{F}\delta\phi_{p,\gamma})(\xi)\|_{L^2}^2+2Re\int_{-\infty}^{\infty}\xi^2(\mathcal{F}\phi_{p-1,\gamma})(\xi)(\mathcal{F}\delta\phi_{p,\gamma})(\xi)d\xi\right).$$

The p order DAHF possesses joint minimal uncertainty in physical and Fourier dual space in the sense that $\phi_{p,\gamma}(x)$ possesses the minimal joint variance, $\|x\phi_{p,\gamma}(x)\|_{L^2}^2\cdot\|\xi(\mathcal{F}\delta\phi_{p,\gamma})(\xi)\|_{L^2}^2$, while also increasing the number of vanishing moments and holding the remainder of the function, $\phi_{p,\gamma}(\cdot)$'s, joint uncertainty constant. Characteristic plots of the DAHF are presented in Figures 5.1 and 5.2.
We also state the properties of the Hermite polynomials relevant here; orthogonality under the Gaussian weight,

$$\int_{-\infty}^{\infty}e^{-x^2}H_m(x)H_n(x)dx = \sqrt{\pi}2^n n!\delta_{n,m},$$

and the decay condition

$$|H_n(x)| < \kappa\sqrt{n!}2^{n/2}e^{x^2/2},$$

where $\kappa \approx 1.09$, [11].

We now undertake a detailed error analysis of a filter, §3, and mollifier, §4, constructed from the DAHF, realizing the optimal values for the localization, γ, and accuracy, p, parameters. By determining the localization parameter γ we obtain the new filter dilation factor of $\sqrt{N/d(x)}$, achieving optimal joint time-frequency localization to $[x-d(x),x+d(x)]\times[-N,N]$. Furthermore, the optimal number of near vanishing moments, p, is selected to balance the accuracy error with the minimized localization errors; yielding the minimal total error.

[3]This is also a direct consequence that either a function or its Fourier transform is analytic, and analytic continuation excludes compact support except for the zero function.

3. Optimal Adaptive order Filter

As stated in Lemma 2.1, the filter

$$\sigma_\gamma(\xi) := e^{-\xi^2\gamma^2/2}\sum_{n=0}^{p}\frac{(\xi^2\gamma^2)^n}{2^n n!}, \tag{3.1}$$

satisfies optimal joint time-frequency localization for the given order, $\sigma_\gamma^{(n)}(0) = \delta_{n,0}$ for $n = 0, 1, \ldots, 2p$. To bound the error after filtering a function's spectral projection with (3.1), we must determine bounds on the physical and dual space localization errors, as well as the accuracy error, (2.4). After constructing these bounds we will determine the optimal localization and moment parameters, γ and p respectively, by balancing the competing error component's decay rates. We begin with the dual space localization error which is bounded by,

$$\begin{aligned}
|L_D(N,p,x)| &:= \|(\psi - S_N\psi) * (f(x) - S_N f(x))\|_{L^\infty} \\
&\leq \|f - S_N f\|_{L^1} \cdot \|\psi - S_N\psi\|_{L^\infty} \\
&\leq Const_f \cdot \sum_{k=N+1}^{\infty}\sigma_\gamma\left(\frac{k}{N}\right) \\
&\leq Const_f \cdot \int_1^\infty \sigma_\gamma(\xi)d\xi \\
&\leq Const_f \cdot \gamma^{-2}p^2\left(\frac{\gamma^2 e}{2p}\right)^p e^{-\gamma^2/2} \qquad (3.2)
\end{aligned}$$

where $Const_f$ is a possibly different constant depending on f. Note that the quantity $(\gamma^2 e/2p)^p$ is maximized at $p = \gamma^2/2$, canceling the exponential decay, $\exp(-\gamma^2/2)$; and as such, for exponential dual space localization to $[-1, 1]$, the filter order must satisfy $p < \gamma^2/2$.

We now turn to the physical space localization error which is controlled by the decay of the filter's associated mollifier. As the filter is dilated by the factor N in the Fourier dual space, its associated mollifier is dilated by $1/N$ in the physical space. Although we do not have an explicit representation of the mollifier formed from the filter's samples, (2.2), the mollifier is directly related to the filter's inverse Fourier Transform. More precisely, the mollifier is constructed from the uniform sampling of the filter, and accordingly the Poisson summation formula states that the dual space sampling corresponds to physical space periodization of the filter's Fourier transform, (2.6),

$$\psi(x) \equiv \sum_{m=-\infty}^{\infty}\phi_{p,\gamma}(N(x + 2\pi m)). \tag{3.3}$$

Before investigating the localization bound for the mollifier, we determine a bound on the filter's Fourier transform,(2.6),

$$\begin{aligned}
|\phi_{p,\gamma}(x)| &\leq e^{-x^2/(2\gamma^2)}\gamma^{-1}\left|\sum_{n=0}^{p}\frac{(-4)^{-n}}{n!}H_{2n}\left(\frac{x}{\gamma\sqrt{2}}\right)\right| \\
&\leq e^{-x^2/(4\gamma^2)}\gamma^{-1}\kappa\sum_{n=0}^{p}\frac{\sqrt{2n!}}{2^n n!} \\
&\leq Const\cdot\gamma^{-1}p^{3/4}e^{-x^2/4\gamma^2}. \qquad (3.4)
\end{aligned}$$

where the sum in the second line is bounded using Sterling's inequality. From relationship (3.3) and the decay of $\phi_{p,\gamma}(x)$ we note that for $|x| \leq \pi$, the mollifier and the filter's Fourier transform are exponentially close,

$$|\psi(x) - \phi_{p,\gamma}(Nx)| \equiv \left|\sum_{m\neq 0}\phi_{p,\gamma}(N(x + 2\pi m))\right| \leq Const\cdot\frac{\gamma p^{3/4}}{N^2}e^{-(\pi N/2\gamma)^2} \qquad |x| \leq \pi, \tag{3.5}$$

and therefore they decay at the same exponential rate, $|\psi(x)| \leq Const|\phi_{p,\gamma}(Nx)|$. Returning to the physical space localization error we obtain the bound,

$$
\begin{aligned}
|L_P(N,p,x)| &:= \left| \int_{r\le|y|\le\pi} [f(x)-f(x-y)]\psi(y)dy \right| \le 2\|f\|_{L^\infty} \int_r^\pi |\psi(y)|dy \\
&\le Const_f \int_r^\pi |\phi_{p,\gamma}(Ny)|\, dy \le Const_f \cdot \frac{\gamma p^{3/4}}{rN^2} e^{-(rN/2\gamma)^2}. \qquad (3.6)
\end{aligned}
$$

With the localization errors quantified we now turn to bounding the accuracy error by determining the number and quality of the associated mollifier's near vanishing moments. As in the case of the physical space localization, we approach this through the properties of the filter's Fourier transform, $\phi_{p,\gamma}(\cdot)$, which possesses $2p+1$ exactly vanishing moments when taken over the entire real line. However, here we are interested in local symmetric moments, defined as

$$
M_{n,r} := \int_{-r}^{r} x^n \psi(x)dx \qquad r \le \pi.
$$

The mollifier possesses exactly vanishing odd moments, we express the even moments for $n \le p$ as

$$
\begin{aligned}
M_{2n,r} &= \int_{-r}^{r} x^{2n}\psi(x)dx - \int_{-\infty}^{\infty} x^{2n}\phi_{p,\gamma}(Nx)dx \\
&= \int_{-r}^{r} x^{2n}[\psi(x)-\phi_{p,\gamma}(Nx)]dx - \int_{|x|>r} x^{2n}\phi_{p,\gamma}(Nx)dx =: \mathcal{M}_1 + \mathcal{M}_2,
\end{aligned}
$$

where the first component is small due to the similarity of the mollifier and the filter's Fourier transform, (3.5)

$$
|\mathcal{M}_1| \le \max_{x\in[-\pi,\pi]} |\psi(x)-\phi_{p,\gamma}(Nx)| \cdot 2\int_0^r x^{2n}dx \le Const \cdot \frac{\gamma p^{3/4}}{N^2} r^{2n} e^{-(\pi N/2\gamma)^2},
$$

and the second is controlled by the physical space localization (3.4)

$$
\begin{aligned}
|\mathcal{M}_2| &\le \int_{|x|>r} x^{2n}|\phi_{p,\gamma}(Nx)|dx \le Const\cdot\gamma^{-1}p^{3/4}\int_r^\infty x^{2n}e^{-(xN/2\gamma)^2}dx \\
&\le Const\cdot\frac{\gamma p^{3/4}}{N^2 r^{1/2}} e^{-(rN/2\gamma)^2} n! \left(\frac{2\gamma}{N}\right)^{2n} \sum_{k=0}^{n} \frac{1}{k!}\left(\frac{rN}{2\gamma}\right)^{2k} \\
&\le Const\cdot\frac{\gamma p^{3/4} n}{N^2 r^{1/2}}\, r^{2n} e^{-(rN/2\gamma)^2} \qquad n \le \left(\frac{rN}{2\gamma}\right)^2.
\end{aligned}
$$

In the above bound for $\mathcal{M}_2$, the sum is initially increasing, reaching is maximum at $k=(rN/2\gamma)^2$; as a result, for $n \le (rN/2\gamma)^2$ the sum reaches its maximized at $k=n$ canceling the term $n!(2\gamma/N)^{2n}$. Combining the bounds for $\mathcal{M}_1$ and $\mathcal{M}_2$, the number and quality of the moments is given by

$$
|M_{2n,r}| \le Const\cdot\frac{p^{3/4}\gamma n}{N^2 r^{1/2}} r^{2n} e^{-(rN/2\gamma)^2} \qquad n \le \left(\frac{rN}{2\gamma}\right)^2. \qquad (3.9)
$$

With near vanishing moments quantified in (3.9), we outline our approach to bounding the accuracy error, $A(N,p,x) := \int_{|y|\le r}[f(x)-f(x-y)]\psi(y)dy$. Traditionally the accuracy error is bounded by Taylor expanding $g_x(y) := [f(x)-f(x-y)]$ about zero and taking the largest symmetric region where $g_x(y)$ is analytic, $r \le d(x)$ where $d(x)$ is the distance from x to the nearest discontinuity of $f(\cdot)$. The canonical Taylor expansion bound is then controlled by the vanishing moments, $M_{2n,r}$, and the truncation of the Taylor expansion, $r^q\|g_x\|_{C^q}/q!$. Here we focus on piecewise analytic functions in which case the Cauchy integral formula quantifies the regularity as

$$
\|f\|_{C^s[x-d(x),x+d(x)]} \le Const\cdot\frac{s!}{\eta_f^s}
$$

where $f(x-z)$ is analytic for the strip in the complex plane, $|\Im(z)| \le \eta_f$, $|x-\Re(z)| \le d(x)$. Incorporating the regularity bound in the classical $q-1$ term truncated Taylor expansion yields a truncation error proportional to $(r/\eta_f)^q$ which is only decreasing for $r < \eta_f$. For a given order spectral projection, optimal joint time-frequency localization in $[x-r, x+r]\times[-N,N]$ requires r selected as large as possible, making the Taylor

expansion bound ineffectual. Alternatively, the Chebyshev expansion of $g_x(\cdot)$ over $[-r,r]$ gives a near min-max approximation for a given order polynomial. Before investigating this alternative Chebyshev polynomial based error decomposition we state relevant results for the Chebyshev polynomials in the following lemma, more general results are cataloged in [14].

Lemma 3.1. *The k^{th} order Chebyshev polynomial is given by*

$$T_k(x) := \sum_{l=0}^{\lfloor k/2 \rfloor} c_l^{(k)} x^{k-2l} \qquad c_l^{(k)} := (-1)^l 2^{k-2l-1} \frac{k}{k-l} \cdot \left(\begin{array}{c} k-l \\ l \end{array} \right)$$

and the Chebyshev expansion of a function, $h(\cdot)$, by

$$S_M^T h(x) := \sum_{k=0}^{M} h_k^T T_k(x) \qquad h_k^T := \frac{2}{\pi} \int_{-1}^{1} \frac{T_k(x) h(x)}{\sqrt{1-x^2}}.$$

The coefficients for a Chebyshev expansion of an analytic function decay exponentially, and as a result, Chebyshev projections converge at an exponential rate

$$|h_k^T| \leq Const_h \cdot \beta_h^{-k} \qquad \Longrightarrow \qquad \max_{|x|\leq 1} |h(x) - S_M^T h(x)| \leq Const_h \beta_h^{-M}, \tag{3.12}$$

where $\beta_h > 1$ is a constant depending on the analytic extension of $h(\cdot)$ to the complex plane. Additionally, the classical three term recursion relationship gives a bound on the growth of the coefficients composing a Chebyshev polynomial

$$c_l^{(k+1)} = 2c_l^{(k)} - c_{l+1}^{(k-1)} \qquad \Longrightarrow \qquad \left| c_l^{(k)} \right| \leq (1+\sqrt{2})^k \quad \forall l.$$

We now turn to bounding the accuracy error, $A(N,p,x)$, decomposed into the two terms

$$\begin{aligned} A(N,p,x) &= \int_{|y|\leq r} \psi(y) g_x(y) dy \\ &= \int_{|y|\leq r} \psi(y) \left(g_x(y) - S_p^T(g_x)(y) \right) dy + \int_{|y|\leq r} \psi(y) S_p^T(g_x)(y) dy =: \mathcal{A}_1 + \mathcal{A}_2 \qquad r \leq d(x), \end{aligned}$$

where the first component is controlled by the decay of Chebyshev coefficients, (3.12), of $g_x(y) := f(x) - f(x-y)$ which is analytic for $r \leq d(x)$,

$$|\mathcal{A}_1| \leq Const_f \cdot \max_{|y|\leq r} |g_x(y) - S_p^T(g_x)(y)| \int_{|y|\leq r} |\psi(y)| dy \leq Const_f \cdot rN\beta_f^{-p}.$$

The second component, $\mathcal{A}_2$ is small for modest p due to the near vanishing moments of the mollifier which correspond to near orthogonality with low order Chebyshev polynomials[4]

$$\begin{aligned} \left| \int_{|y|\leq r} T_{2k}\left(\frac{y}{r}\right) \psi(y) dy \right| &\leq \sum_{l=0}^{k} r^{2(l-k)} \left| c_l^{(2k)} \right| \cdot \left| M_{2(k-l),r} \right| \leq (1+\sqrt{2})^{2k} \sum_{j=0}^{k} r^{-2j} |M_{2j,r}| \\ &\leq Const \cdot \frac{p^{3/4} k^2 \gamma}{N^2 r^{1/2}} (1+\sqrt{2})^{2k} e^{-(rN/2\gamma)^2} \qquad k \leq \left(\frac{rN}{2\gamma} \right)^2, \end{aligned}$$

[4]We only consider the even Chebyshev polynomials as the mollifier is even, giving exact orthogonality to all odd functions.

resulting in the bound

$$\begin{aligned}
|\mathcal{A}_2| &= \left| \int_{|y|\le r} \psi(y) S_p^T(g_x)(y) dy \right| \\
&= \left| \sum_{k=0}^{p} (g_x)_k^T \int_{|y|\le r} T_k\left(\frac{y}{r}\right) \psi(y) dy \right| \\
&\le Const_f \sum_{k=0}^{\lfloor p/2 \rfloor} \beta_f^{-2k} \left| \int_{|y|\le r} T_{2k}\left(\frac{y}{r}\right) \psi(y) dy \right| \\
&\le Const_f \frac{p^{15/4}\gamma}{N^2 r^{1/2}} e^{-(rN/2\gamma)^2} \left(1 + \left(\frac{1+\sqrt{2}}{\beta_f}\right)^p\right).
\end{aligned}$$

Combining the bounds for $\mathcal{A}_1$ and $\mathcal{A}_2$ yields the total accuracy error bound,

$$|A(N,p,x)| \le Const_f \cdot rN\beta_f^{-p} + Const_f \frac{p^{15/4}\gamma}{N^2 r^{1/2}} e^{-(rN/2\gamma)^2} \left(1 + \left(\frac{1+\sqrt{2}}{\beta_f}\right)^p\right). \tag{3.15}$$

Now that the different error components $(L_D,\ L_P,\ A)(N,p,x)$ have been bounded we arrive at the overall error bound,

$$|f(x) - S_N f^\sigma(x)| \le Const_f \left[rN\beta_f^{-p} + C_1 e^{-\gamma^2/2} + C_2 e^{-(rN/2\gamma)^2} \right] \tag{3.16}$$

with functions

$$C_1 := \left(\frac{p}{\gamma}\right)^2 \left(\frac{\gamma^2 e}{2p}\right)^p, \qquad C_2 := \frac{\gamma p^{3/4}}{rN^2} + \frac{p^{15/4}\gamma}{N^2 r^{1/2}} \left(1 + \left(\frac{1+\sqrt{2}}{\beta_f}\right)^p\right). \tag{3.17}$$

The optimal behavior of the localization and accuracy parameters, γ and p respectively, are selected so that the competing error components possess the same decay rate, with the dominant error components given by β_f^{-p}, $\exp(-\gamma^2/2)$, and $\exp(-(rN/2\gamma)^2)$. Although the optimal values of γ and p depend on the particular function being approximated through β_f, the decay rates can be balanced by equating, $p = \gamma^2/2 = (rN/2\gamma)^2$, resulting in

$$\gamma := \sqrt{\alpha rN} \qquad p := \kappa rN. \tag{3.18}$$

With these relationships we return to the second and third components of the overall error, as expressed in equation (3.16), fully including the growth rate of C_1 and C_2. For the parameters selected as described in (3.18), the second component is bounded by,

$$C_1 e^{-\gamma^2/2} = \frac{\kappa^2}{\alpha} rN \left(\frac{2\kappa^\kappa e^{\alpha/2}}{(\alpha e)^\kappa}\right)^{-rN},$$

and the third error element simplifies to

$$\begin{aligned}
C_2 e^{-(rN/2\gamma)^2} &\le Const \cdot r^{15/4} N^{9/4} \left(1 + \left(\frac{\beta_f}{1+\sqrt{2}}\right)^{-\kappa rN}\right) e^{-\frac{1}{2\alpha} rN} \\
&\le Const \cdot r^{15/4} N^{9/4} \left(\frac{e^{1/2\alpha}}{(1+\sqrt{2})^\kappa}\right)^{-rN},
\end{aligned}$$

where the second line is due to $\beta_f > 1$ for $f(\cdot)$ piecewise analytic. Exponential decay in rN of the second and third component then requires $(\alpha e/\kappa)^\kappa / 2e^{\alpha/2} < 1$, and $\exp(1/2\alpha)(1+\sqrt{2})^{-\kappa} > 1$ respectively.
In all of the above bounds, the exponential convergence rate is gained through the factor rN, which for a given projection order, N, obtains its largest value for $r = d(x)$ where $d(x)$ is the distance from the point x to the nearest discontinuity in $f(\cdot)$. The localization and accuracy parameters are then given adaptively by

$$\gamma := \sqrt{\alpha N d(x)} \qquad \text{and } p := \kappa N d(x). \tag{3.20}$$

The above bounds are summarized in the following theorem:

Theorem 3.2. *Given the N truncated Fourier coefficients, of a piecewise analytic function, $\{\hat{f}_k\}_{|k|\le N}$, the function can be recovered within the exponential bound*

$$\left| f(x) - \frac{1}{2\pi} \sum_{|k|\le N} \sigma_{opt}\left(k, N, x\right) \hat{f}_k e^{ikx} \right| \le Const_f \cdot N^{9/4} \tau^{-Nd(x)} \tag{3.21}$$

where $\tau := \min\left(\beta_f^k, 2e^{\alpha/2}\left(\frac{\kappa}{\alpha e}\right)^{\kappa}, \frac{e^{1/2\alpha}}{(1+\sqrt{2})^{\kappa}}\right)$ *and with the adaptive filter*

$$\sigma_{opt}\left(k, N, x\right) := e^{\frac{\alpha k^2 d(x)}{2N}} \sum_{n=0}^{\lfloor \kappa N d(x) \rfloor} \frac{1}{n!}\left(\frac{\alpha k^2 d(x)}{2N}\right)^n. \tag{3.22}$$

The optimal values for the free constants, α and κ, depend on the function's regularity constant[5], β_f. None the less, numerical experiments encourage a relatively small value for κ, making the dominant contributions from the localization constant given by $e^{\alpha/2}$ and $e^{1/2\alpha}$, which are balanced for $\alpha = 1$. Numerical experiments then indicate that selecting $\kappa = 1/15$ gives good results for a variety of functions with significantly different regularity constants; for these selections, τ reduces to

$$\tau = \min\left(1.55, \beta_f^{1/15}\right) \qquad \text{with} \quad \alpha = 1, \quad \kappa = 1/15. \tag{3.23}$$

Unlike classical filters which are dilated by N, to maximize the localization for the time-frequency domain $[x - d(x), x + d(x)] \times [-N, N]$, the localization parameter, $\gamma = \sqrt{Nd(x)}$, yields the optimal filter which is dilated by $\sqrt{N/d(x)}$. In the following section we construct the optimal mollifier defined in the physical space, arriving at the dilation rate $\sqrt{d(x)/N}$, in contrast to traditional mollifiers which are dilate by $d(x)$. Consequently, the optimal filter and mollifier satisfy dilation relationships which are the inverse of each other, as the Fourier transform implies, but which is not satisfied for classical filters and mollifiers.

4. Optimal Adaptive order Mollifier

Rather than a function's spectral projection, $S_N f$, the function's pseudo-spectral information can be given in the form of its equidistant samples, $f(y_\nu)$ where $y_\nu := \frac{\pi}{N}(\nu - N)$ for $\nu = 0, 1, \ldots, 2N-1$. The function's trigonometric interpolant is formed from these samples,

$$I_N f(x) := \sum_{|k|\le N} \tilde{f}_k e^{ikx} \qquad \tilde{f}_k := \frac{\pi}{N} \sum_{\nu=0}^{2N-1} f(y_\nu) e^{-iky_\nu},$$

where the pseudo-spectral coefficients, $\tilde{f}_k$, are an approximation of the true Fourier coefficient, $\hat{f}_k$; replacing the integral in (2.1) with its trapezoidal sum. Although for piecewise smooth functions the trapezoidal quadrature is only first order, $|\tilde{f}_k - \hat{f}_k| \approx \mathcal{O}(N^{-1})$, the function can be approximated within the same bound as presented in Theorem 3.2. This approximation may be implemented either by filtering the trigonometric interpolant, or entirely in the physical space through a discrete convolution with a mollifier,

$$I_N f^\sigma(x) := \psi * I_N f(x) \equiv \frac{1}{2\pi} \sum_{|k|\le N} \sigma\left(\frac{k}{N}\right) \tilde{f}_k e^{ikx} \equiv \frac{\pi}{N} \sum_{\nu=0}^{2N-1} f(y_\nu) S_N\psi(x - y_\nu). \tag{4.2}$$

We now conduct a short analysis proving the filtered interpolant yields an approximation within the same bound as that given in Theorem 3.2.
An error decomposition similar to (2.4) is satisfied for the filtered trigonometric interpolant

$$\begin{aligned} \tilde{E}(N,p,x) &:= f(x) - \psi * I_N f(x) \\ &= (f(x) - \psi * f(x)) + (\psi - S_N\psi) * (f(x) - I_N f(x)) \\ &=: R(N,p,x) + \tilde{L}_D(N,p,x) \equiv \tilde{L}_D(N,p,x) + L_P(N,p,x) + A(N,p,x), \end{aligned} \tag{4.3}$$

[5]Here we concern ourselves with near optimal function independent estimates, but note that the convergence rate for a given function may be increased if β_f were approximated, [5].

where the physical space localization and accuracy errors are unchanged from the spectral projection error expansion. For the modified dual space localization error we follow the same steps as for the original dual space localization error, (3.2),

$$\begin{aligned}\left|\tilde{L}_D(N,p,x)\right| &:= \|(\psi - S_N\psi) * (f(x) - I_N f(x))\|_{L^\infty} \\ &\leq \|f - I_N f\|_{L^1} \cdot \|\psi - S_N\psi\|_{L^\infty} \\ &\leq Const_f \cdot \sum_{k=N+1}^{\infty} \sigma_\gamma\left(\frac{k}{N}\right) \\ &\leq Const_f \cdot \int_1^\infty \sigma_\gamma(\xi)d\xi \\ &\leq Const_f \cdot \gamma^{-2}p^2\left(\frac{\gamma^2 e}{2p}\right)^p e^{-\gamma^2/2}. \qquad (4.4)\end{aligned}$$

Combining the modified dual space localization bound, (4.4) with the unchanged physical space localization and accuracy bounds, (3.6) and (3.15) respectively, yields the same composite error bound as for the filtered spectral projection, equation (3.16). The optimal filter parameters are then selected in the same fashion; resulting in a convergence rate of the same order as in Theorem 3.2.

Theorem 4.1. *Given the $2N$ equidistant samples, of a piecewise analytic function, $\{f(\frac{\pi}{N}(\nu - N))\}_{\nu=0}^{2N-1}$, the function can be recovered within the exponential bound*

$$\left| f(x) - \frac{1}{2\pi}\sum_{|k|\leq N} \sigma_{opt}(k,N,x)\tilde{f}_k e^{ikx}\right| \leq Const_f \cdot N^{9/4}\tau^{-Nd(x)}$$

where τ and the adaptive filter are given in Theorem 3.2.

As stated earlier, alternatively to filtering the trigonometric interpolant, the same approximation can be implemented as a discrete physical space convolution with the mollifier $S_N\psi(\cdot)$, (4.2). Although the samples are given in the physical space, and the implementation is also conducted in the physical space, this mollifier is defined in terms of the dual space filter $\sigma_{opt}(\cdot)$. We now construct a mollifier defined in the physical space, using the optimal order filter's inverse Fourier transform, $\phi_{p,\gamma}(N\cdot)$, which was shown to be exponentially close to the optimal filter's associated mollifier, (3.5). With such a mollifier defined entirely in the physical space, a piecewise smooth function can be approximated from its equidistant samples through a purely physical space implementation. We now detail the error analysis for the mollifier, $\phi_{p,\gamma}(N\cdot)$, proving that the overall convergence rate in Theorem 4.1 is not adversely effected by replacing the dual space constructed mollifier $S_N\psi(\cdot)$ with physical space mollifier $\phi_{p,\gamma}(N\cdot)$.

Unlike the filter's associated mollifier, $\psi(\cdot)$, the mollifier defined directly in the physical space, $\phi_{p,\gamma}(N\cdot)$, is not periodic, and as such the implementation requires the periodic extension of the samples,

$$f_\pi(y_\nu + 2\pi n) := f(y_\nu) \qquad \text{for} \quad n = -1, 0, 1.$$

Furthermore we define the symmetric region surrounding x as $I_{x,u} := (x-u, x+u]$. The mollifier can either be applied to the entire $2N$ distinct samples contained in $I_{x,\pi} =: I_x$, or to those points in the largest symmetric smooth region by restricting to $I_{x,d(x)}$, where an additional physical space localization error is introduced. In the following analysis we use the full set of points, but note that the additional error when using $I_{x,d(x)}$ does not effect the overall convergence rate, and as discussed in §5, with proper normalization allows for improved first order accuracy in the immediate neighborhood of the discontinuity.

The error after discrete mollification with $\phi_{p,\gamma}(N\cdot)$ is defined, and can be expanded as follows:

$$\begin{aligned}E_{mol}(N,p,x) &:= f(x) - \frac{\pi}{N}\sum_{y_\nu\in I_x} f_\pi(y_\nu)\phi_{p,\gamma}(N(x-y_\nu)) \\ &= f(x) - \frac{\pi}{N}\sum_{y_\nu\in I_x} f_\pi(y_\nu)S_N\psi(x-y_\nu) + \frac{\pi}{N}\sum_{y_\nu\in I_x} f_\pi(y_\nu)[S_N\psi(x-y_\nu) - \psi(x-y_\nu)] \\ &+ \frac{\pi}{N}\sum_{y_\nu\in I_x} f_\pi(y_\nu)[\psi(x-y_\nu) - \phi_{p,\gamma}(N(x-y_\nu))] \\ &=: \mathcal{E}_1 + \mathcal{E}_2 + \mathcal{E}_3. \qquad (4.7)\end{aligned}$$

The first component is simply the error when filtering the trigonometric interpolant,

$$\mathcal{E}_1 := f(x) - \frac{\pi}{N} \sum_{y_\nu \in I_x} f_\pi(y_\nu) S_N \psi(x - y_\nu) = f(x) - \psi * I_N f(x),$$

with the last equality due to $\psi(\cdot)$ being 2π periodic, so that the sum over I_x is the same as over $\nu = 0, 1, \ldots, 2N-1$. The bound for $\mathcal{E}_1$ is given in Theorem 4.1, and is composed of the elements in equation (4.3).

The second component of E_{mol} satisfies the same bound as the dual space localization error, $L_D(N,p,x)$,

$$\begin{aligned} |\mathcal{E}_2| &= \frac{\pi}{N} \left| \sum_{y_\nu \in I_x} f_\pi(y_\nu) [S_N \psi(x - y_\nu) - \psi(x - y_\nu)] \right| \\ &\leq 2\pi \|f\|_{L^\infty[-\pi,\pi]} \|\psi - S_N \psi\|_{L^\infty} \\ &\leq Const_f \sum_{|k|>N} \sigma \frac{k}{N} \leq Const_f \int_1^\infty \sigma(\xi) d\xi \\ &\leq Const_f \left(\frac{p}{\gamma}\right)^2 \left(\frac{\gamma^2 e}{2p}\right)^p e^{-\gamma^2/2}, \end{aligned}$$

and the third component is controlled by the different mollifiers, $\psi(\cdot)$ and $\phi_{p,\gamma}(N\cdot)$, being exponentially close as quantified in equation (3.5)

$$\begin{aligned} |\mathcal{E}_3| &= \frac{\pi}{N} \left| \sum_{y_\nu \in I_x} f_\pi(y_\nu) [\psi(x - y_\nu) - \phi_{p,\gamma}(N(x - y_\nu))) \right| \\ &\leq 2\pi \|f\|_{L^\infty[-\pi,\pi]} \cdot \|\psi(z) - \phi_{p,\gamma}(Nz)\|_{L^\infty[-\pi,\pi]} \\ &\leq Const_f \, \frac{\gamma p^{3/4}}{N^2} e^{-(\pi N/2\gamma)^2}. \end{aligned}$$

Combining the above bounds we achieve the same overall bound as for the filtered spectral projection,

$$\begin{aligned} |E_{mol}(N,p,x)| &\leq |f(x) - \psi * I_N f(x)| + Const_f \left[\left(\frac{p}{\gamma}\right)^2 \left(\frac{\gamma^2 e}{2p}\right)^p e^{-\gamma^2/2} + \frac{\gamma p^{3/4}}{N^2} e^{-(\pi N/2\gamma)^2} \right] \\ &\leq Const_f \left[r N \beta_f^{-p} + C_1 e^{-\gamma^2/2} + C_2 e^{-(rN/2\gamma)^2} \right] \end{aligned}$$

where C_1 and C_2 are defined in equation (3.17). As this is the same bound as was achieved for filtering the spectral projection, (3.16), the localization and accuracy parameters are selected in the same fashion as for the optimal adaptive order filter, $\gamma := \sqrt{\alpha N d(x)}$ and $p := \kappa N d(x)$. The above results are summarized in the following theorem:

Theorem 4.2. *Given the $2N$ equidistant samples, of a piecewise analytic function, $\{f(\frac{\pi}{N}(\nu - N))\}_{\nu=0}^{2N-1}$, the function can be recovered within the exponential bound*

$$\left| f(x) - \frac{\pi}{N} \sum_{y_\nu \in I_x} f_\pi(y_\nu) \phi_{opt}(N(x - y_\nu)) \right| \leq Const_f \cdot N^{9/4} \tau^{-N d(x)}$$

where $\tau := \min\left(\beta_f^k, 2e^{\alpha/2} \left(\frac{\kappa}{\alpha e}\right)^\kappa, \frac{e^{1/2\alpha}}{(1+\sqrt{2})^\kappa}\right)$, and the mollifier is given by

$$\phi_{opt}(N,x) := \frac{1}{\sqrt{N d(x)}} \exp\left(\frac{N x^2}{2 d(x)}\right) \sum_{n=0}^{\lfloor N d(x)/15 \rfloor} \frac{4^{-n}}{n!} H_{2n}\left(x \sqrt{\frac{N}{2 d(x)}}\right). \tag{4.10}$$

Again we select the parameter constants as $\alpha = 1$ and $\kappa = 1/15$ for the simplified value of τ in equation (3.23). Unlike the adaptive filter and mollifier of [18] and [17], modulo exponentially small differences, the optimal filter and mollifier are performing the same action in the different frequency (dual) and physical spaces. This is reflected in the mollifier dilation factor $\sqrt{d(x)/N}$ which is the inverse of the filter's dilation rate, as the Fourier transform would imply.

5. Numerical Examples

For the following example we contrast the optimal adaptive filter, $\sigma_{opt}(\cdot)$, and mollifier, $\phi_{opt}(\cdot)$, presented in Theorems 3.2 and 4.2 with the more traditional compactly supported adaptive filter and mollifier constructed and analyzed in [18] and [17],

$$\sigma_{adapt}(\xi) := \begin{cases} e^{\left(\frac{c_q \xi^q}{\xi^2-1}\right)} & |\xi| < 1 \\ 0 & |\xi| \geq 1 \end{cases}, \qquad c_q := 2^q \frac{3}{8} \cdot \frac{18q^2+3q+14}{9q^2+6q+2}, \tag{5.1}$$

$$\psi_{adapt}(x) := \begin{cases} \frac{2}{d(x)} \frac{\sin\left((p(x)+1)\frac{\pi x}{d(x)}\right)}{\sin\left(\frac{\pi x}{2d(x)}\right)} \exp\left(\frac{10x^2}{x^2-d(x)^2}\right) & |x| < d(x) \\ 0 & |x| \geq d(x) \end{cases}, \tag{5.2}$$

with adaptive orders, $q(x) := \max\left(2, \frac{1}{2}\sqrt{Nd(x)}\right)$, and $p(x) := Nd(x)/\pi\sqrt{e}$. In [18] and [17] it was shown that the above compactly supported filter and mollifier satisfy theorems similar to Theorems 3.2 and 4.2, but with the root exponential convergence rate, $\exp(-\eta_f\sqrt{Nd(x)})$ for some $\eta_f > 0$ depending on the particular function being filtered. The optimal filter and mollifier achieve superior, true exponential accuracy by not imposing compact support in the dual or physical space respectively; rather, they satisfy optimal joint time-frequency localization to $[x-d(x), x+d(x)] \times [-N, N]$. Figure 5.1 illustrates the adaptive filter of [18] and the optimal filter for a fixed value spectral projection order, N, and various values of $d(x)$.

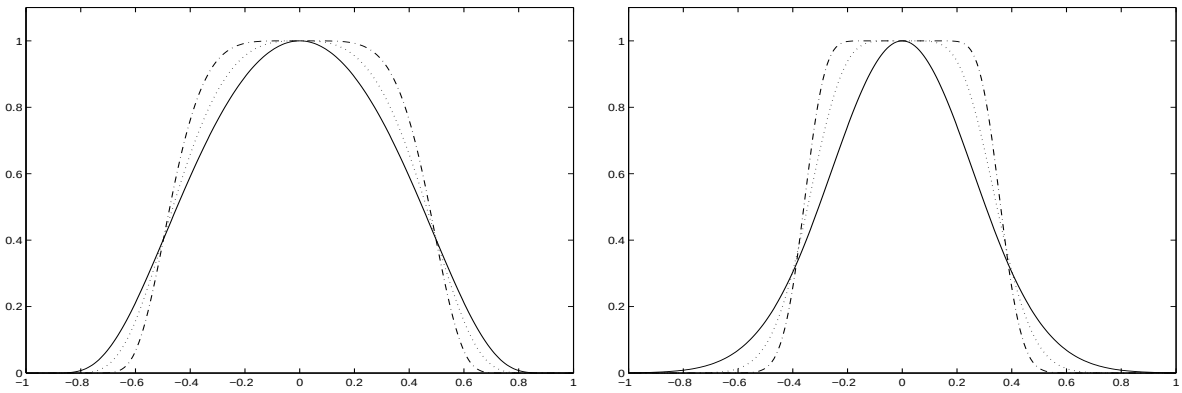

Figure 5.1: The compactly supported adaptive filter (5.1) shown left, and optimal filter (3.22) seen right, for $N = 128$, and $d(x) = 3^{(n-3)}\pi$ with $n = 0, 1, 2$, solid, dotted, and dashed respectively. The resulting adaptive filter orders are, $q = 2, 3, 5$ and the optimal filter of order $2p$ with $p = 0, 2, 8$.

Figure 5.2 shows the mollifiers associated with the optimal adaptive order filter, σ_{opt}, shown in Figure 5.1(right). As the filter order increases, the number of near vanishing moments increases, exhibited through increased oscillations, as well as the asymptotic physical space localization, but at the cost of decreased initial localization. Selecting the optimal filter parameters as (3.20), the optimal filter (3.22) balances these competing behaviors, resulting in the minimal error as decomposed in (2.4).

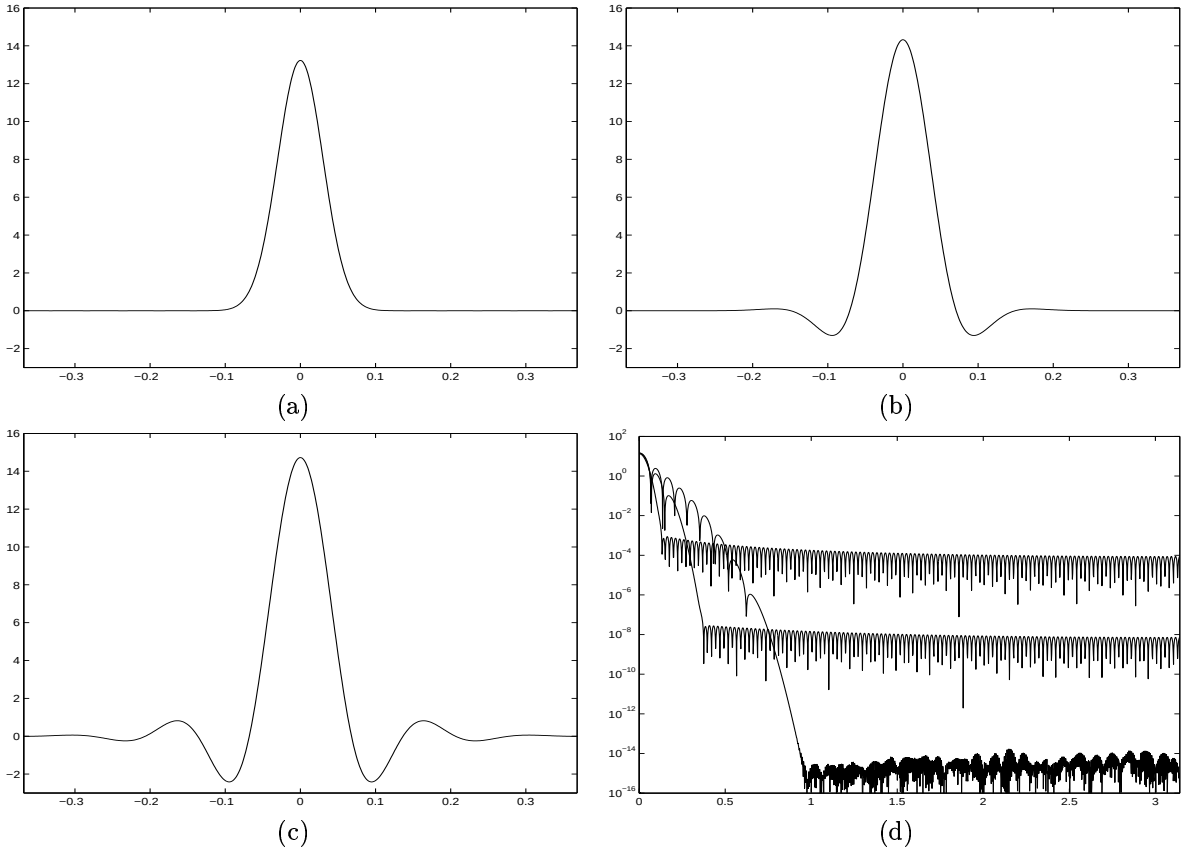

Figure 5.2: The optimal filter $\sigma_{opt}(\cdot)$'s associated mollifier for $N = 128$ and $d(x) = 3^{(n-3)}\pi$ in (a-c) for $n = 0, 1, 2$ respectively; and the log of the same mollifiers (d) with increasing asymptotic decay for increasing $d(x)$.

The following numerical examples are conducted for the function

$$f(x) = \begin{cases} (2e^{2x} - 1 - e^{\pi})/(e^{\pi} - 1) & x \in [0, \pi/2) \\ -\sin(2x/3 - \pi/3) & x \in [\pi/2, 2\pi) \end{cases}, \tag{5.3}$$

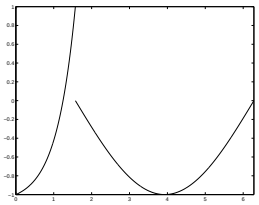

which was constructed as a challenging test problem with a large gradient to the left of the discontinuity at $x = \pi/2$. Moreover, lacking periodicity $f(\cdot)$ feels three discontinuities per period;

$$d(x) = min(|x|, |x - \pi/2|, |x - 2\pi|) \quad x \in [0, 2\pi],$$

and has substantially different regularity constants for the two functions composing it.
In Figure 5.3 the exact Fourier coefficients, $\{\hat{f}_k\}_{k \le N}$, are given and then filtered to approximate $f(x)$. Although the adaptive filter achieves exponential convergence, Figure 5.3(c), it is at a substantially slower rate than is realized by the optimal order filter, Figure 5.3(d). For the optimal filter the convergence in the immediate neighborhood of the discontinuities is also improved as illustrated in the removal of small oscillations seen in Figure 5.3(a) but not 5.3(b).

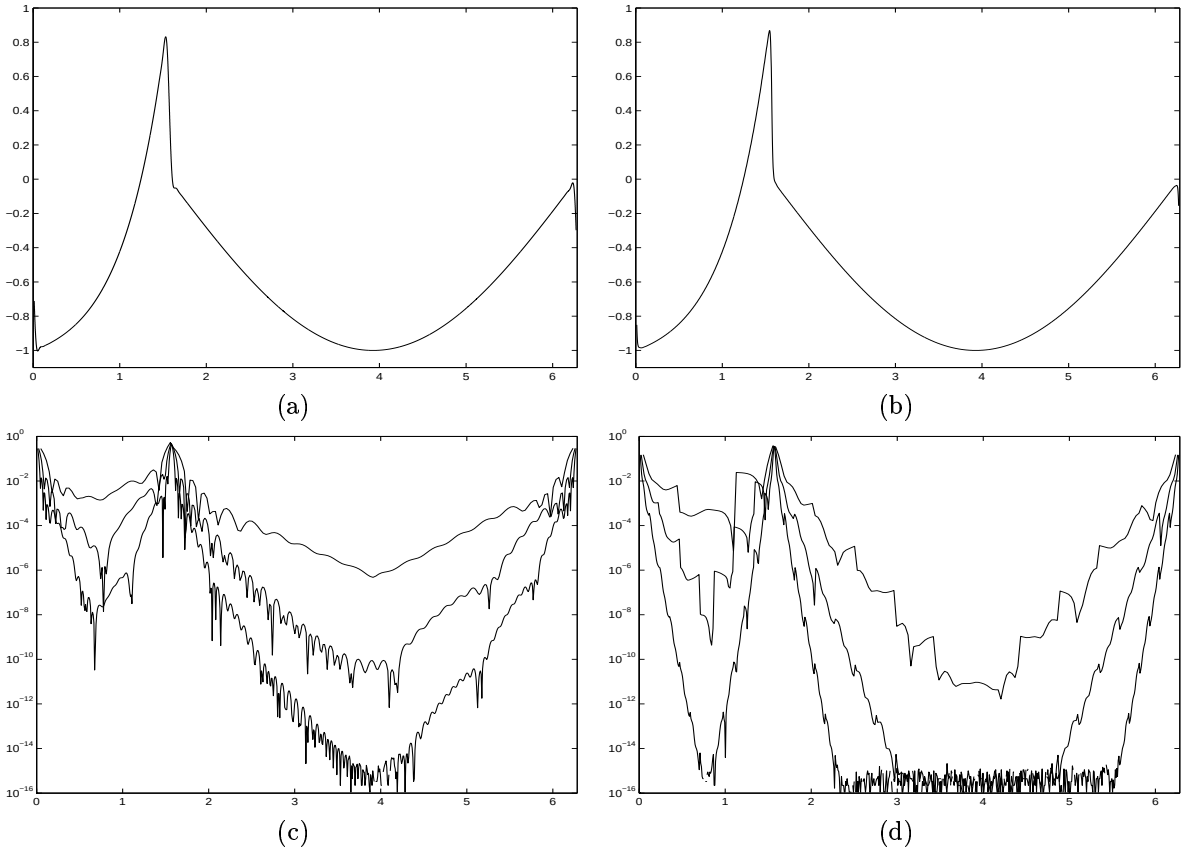

Figure 5.3: The filtered 128 mode spectral projection using the adaptive filter (5.1) and optimal filter (3.22), (a) and (b) respectively. The error in the reconstructions for $N = 32, 64, 128$ for the adaptive filter (c) and optimal filter (d).

Figure 5.4 contrasts the adaptive mollifier of [17] with the optimal mollifier, (4.10), where the function $f(x)$ is approximated from its $2N$ equidistant samples over $[0, 2\pi)$, through discrete physical space convolution. The optimal adaptive order mollifier yields a nearly indistinguishable asymptotic convergence rate as the optimal filter, Figures 5.3(d) and 5.4(d), and the optimal mollifier substantially out performs the adaptive mollifier, (5.2), as contrasted in Figures 5.4(c,d). For the above computations the optimal mollifier is applied to only the samples in the symmetric interval, $I_{x,d(x)} = [x - d(x), x + d(x)]$, and both mollifiers are normalized to possess exact unit mass, i.e. the zeroth moment. By further limiting their support to contain at least two samples, $d(x) := \max(d(x), \pi/N)$, this normalization results in at least first order approximations, significantly reducing the blurring in the immediate $\mathcal{O}(1/N)$ neighborhood of the discontinuities, as contrasted in Figure 5.3(a,b) and 5.4(a,b). A full discussion of this normalization is given in [17]. No similar method to enforce first order accuracy up to the discontinuities is known for filters defined in the Fourier dual space.

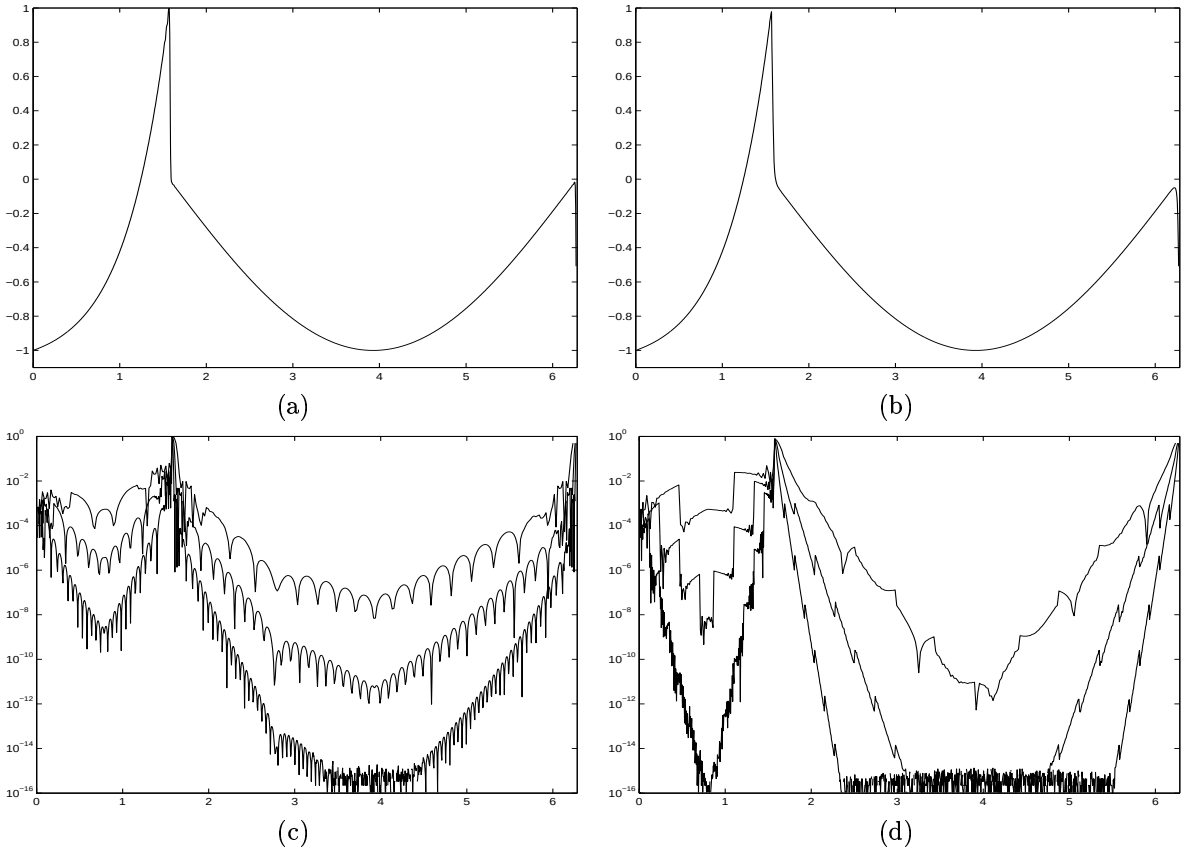

Figure 5.4: The mollified 128 mode spectral projection using the adaptive mollifier (5.2) and optimal mollifier (4.10), (a) and (b) respectively. The error in the reconstructions for $N = 32, 64, 128$ for the adaptive mollifier (c) and optimal mollifier (d).

Summary

Before summarizing the properties of the optimal filter and mollifier, to better put them in context we review some of the more recent significant advances in the development of filters, a more detailed historical account is given in [10]. Shortly after Gibbs' phenomena was discovered, filters were constructed to regain the rapid convergence associated with Fourier projections of smooth functions, in the context of piecewise smooth functions. Beginning with Fejér in 1900 a host of polynomial order filters were introduced, culminating in the infinite order filter of [15], which satisfies (1.3) for q arbitrarily large, yet which gives inferior convergence near discontinuities. With the goal of recovering a convergence rate faster than any polynomial order, spectral accuracy, Gottlieb and Tadmor introduced the compactly supported spectral mollifier of [10], with the number of near vanishing moments selected as a power of the projection order, N^α for $\alpha \approx 1/2$; additionally, for localization to the largest symmetric smooth region, the spectral mollifier was dilated in the physical space by the distance to the nearest discontinuity, $d(x)$. Later, Vandeven introduced the spectral filter, which following the form of other classical compactly supported filters is dilated in the dual space by the projection order, N, and similar to the spectral mollifier selects the number of near vanishing moments as a power of N, [19]. Recently it has been determined that for filters and mollifiers satisfying these classical dilation relationships, $d(x)$ and N in the dual (frequency) and physical (time) space respectively, the optimal number of near vanishing moments should be selected adaptively as a function both N and $d(x)$, [17, 18]; resolving the methodology that the order should decrease when approaching discontinuities, [1, 2]. However, although filters and mollifiers have often been viewed as implementations of the same action in the different dual (frequency) and physical (time) spaces, their dilation parameters are not the inverse of each other, as the Fourier transform would imply.

In this work we discard the classical restriction of compact support, and use the theory of time-frequency analysis to construct a filter and mollifier with optimal joint time-frequency localization to the region dictated

by the function's smoothness, and the projection order, $[x - d(x), x + d(x)] \times [-N, N]$. This analysis results in the new fundamental dilation relationship $\sqrt{N/d(x)}$ and its inverse in the dual and physical spaces respectively. Furthermore, similar to [17, 18] the number of near vanishing moments is selected to balance the accuracy and localization errors, again determined to be a function of both localization parameters N and $d(x)$. In addition to very substantial improvements in the convergence rate, as reflected in Theorems 3.2 and 4.2 as well as Figures 5.3 and 5.4, the optimal filter and mollifier are robust to inaccuracies in the calculation of $d(x)$. Using an incorrect values of $d(x)$ does not destroy the accuracy for the entire smooth region, rather a sub-optimal exponential accuracy is realized due to the imbalance of the localization and accuracy errors. In conclusion, the optimal filter and mollifier presented here are a robust, exponentially accurate, and computationally efficient method for the manipulation of piecewise smooth functions, given its spectral information.

Acknowledgments

I would like to thank Thomas Strohmer for the introduction to Hermite Distributed Approximating Functionals, as well as to thank Eitan Tadmor and David Gottlieb for many informative discussions on the resolution of Gibbs' phenomena.

References

1. J. P. Boyd *A Lag-Averaged Generalization of Euler's Method for Accelerating Series*, Appl. Math. Comput., (1995) 143-166.
2. J. P. Boyd *The Erfc-Log Filter and the Asymptotics of the Euler and Vandeven Sequence Accelerations*, Proceedings of the Third International Conference on Spectral and High Order Methods, (1996) 267-276.
3. A. Gelb, *The resolution of the Gibbs phenomenon for spherical harmonics*, Math. Comp., 66 (1997), 699-717.
4. A. Gelb, *A Hybrid Approach to Spectral Reconstruction of Piecewise Smooth Functions*, Journal of Scientific Computing, October 2000.
5. A. Gelb and Zackiewicz, *Determining Analyticity for Parameter Optimizaion of the Gegenbauer Reconstruction Method*, preprint.
6. A. Gelb and E. Tadmor, *Detection of Edges in Spectral Data*, Applied Computational Harmonic Analysis 7, (1999) 101-135.
7. A. Gelb and E. Tadmor, *Detection of Edges in Spectral Data II. Nonlinear Enhancement*,SIAM Journal of Numerical Analysis, 38 (2000), 1389-1408.
8. D. Gottlieb and C.-W. Shu, *On The Gibbs Phenomenon IV: recovering exponential accuracy in a sub-interval from a Gegenbauer partial sum of a piecewise analytic function*, Math. Comp., 64 (1995), 1081-1095.
9. D. Gottlieb and C.-W. Shu, *On the Gibbs phenomenon and its resolution*, SIAM Review 39 (1998), 644-668.
10. D. Gottlieb and E. Tadmor, *Recovering pointwise values of discontinuous data within spectral accuracy*, in "Progress and Supercomputing in Computational Fluid Dynamics", Proceedings of 1984 U.S.-Israel Workshop, Progress in Scientific Computing, Vol. 6 (E. M. Murman and S. S. Abarbanel, eds.). Birkhauser, Boston, 1985, 357-375.
11. I. Gradshteyn and I. Ryzhik, Table of Integrals, Series, and Products, Academic Press, 2000.
12. K. Gröchenig, Foundations of Time-Frequency Analysis, Birkhäuser, Boston, 2001.
13. D.K. Hoffman and D.J. Kouri, *Hierarchy of Local Minimum Solutions of Heisenberg's Uncertainty Principle*, Phy. Rev. Lett. 25 (2002), 5263-7.
14. J.C. Mason and D.C. Handscomb, Chebyshev Polynomials, Chapman & Hall/CRC, New York, 2003.
15. A. Majda, J. McDonough and S. Osher, *The Fourier method for nonsmooth initial data*, Math. Comput. 30 (1978), 1041-1081.
16. E. Tadmor, *Spectral Methods for Hyperbolic Problems*, from "Lecture Notes Delivered at Ecole Des Ondes", January 24-28, 1994. Available at http://www.math.ucla.edu/~tadmor/pub/spectral-approximations/Tadmor.INRIA-94.pdf
17. E. Tadmor and J. Tanner, *Adaptive Mollifiers - High Resolution Recovery of Piecewise Smooth Data from its Spectral Information*, J. Foundations of Comp. Math. 2 (2002), 155-189.
18. E. Tadmor and J. Tanner, *Adaptive Filters for Piecewise Smooth Spectral Data*, submitted to IMA J. Numerical Analysis.
19. H. Vandeven, *Family of Spectral Filters for Discontinuous Problems*, Journal of Scientific Computings, V6 No2 (1991), 159-192.

Department of Statistics, Stanford University, Stanford, CA 94305-9025
Current address: Department of Mathematics, University of California Davis, Davis, CA 95616
E-mail address: jtanner@math.ucdavis.edu